

















RESEARCH ARTICLE

Multimodal testing reveals subclinical neurovascular dysfunction in prediabetes, challenging the diagnostic threshold of diabetes

Varo Kirthi^{1,2}  | Kate I. Reed²  | Komeil Alattar¹  | Benjamin P. Zuckerman¹  |
Catey Bunce³  | Paul Nderitu^{1,2}  | Uazman Alam^{4,5,6}  | Bronagh Clarke⁷ |
Scott Hau^{7,8}  | Fatima Al-Shibani⁹  | Ioannis N. Petropoulos⁹  |
Rayaz A. Malik^{6,9}  | Theodoros Pissas^{1,8}  | Christos Bergeles¹  |
Prashanth Vas^{1,2}  | David Hopkins^{1,2}  | Timothy L. Jackson^{1,2} 

¹King's College London, London, UK

²King's College Hospital NHS Foundation Trust, London, UK

³Biomedical Research Centre, The Royal Marsden NHS Foundation Trust and the Institute of Cancer Research, London, UK

⁴University of Liverpool, Liverpool, UK

⁵Liverpool University Hospitals NHS Foundation Trust, Liverpool, UK

⁶Institute of Cardiovascular Sciences, Cardiac Centre, Faculty of Medical and Human Sciences, University of Manchester, Manchester, UK

⁷Moorfields Eye Hospital NHS Foundation Trust, London, UK

⁸University College London, London, UK

⁹Division of Research, Weill Cornell Medicine-Qatar, Doha, Qatar

Correspondence

Varo Kirthi, Department of Ophthalmology, Faculty of Life Sciences and Medicine, Normanby Building, King's College Hospital, London SE5 9RS, UK.
Email: v.kirthi@nhs.net

Abstract

Aim: To explore if novel non-invasive diagnostic technologies identify early small nerve fibre and retinal neurovascular pathology in prediabetes.

Methods: Participants with normoglycaemia, prediabetes or type 2 diabetes underwent an exploratory cross-sectional analysis with optical coherence tomography angiography (OCT-A), handheld electroretinography (ERG), corneal confocal microscopy (CCM) and evaluation of electrochemical skin conductance (ESC).

Results: Seventy-five participants with normoglycaemia ($n = 20$), prediabetes ($n = 29$) and type 2 diabetes ($n = 26$) were studied. Compared with normoglycaemia, mean peak ERG amplitudes of retinal responses at low (16-Td-s: $4.05 \mu\text{V}$, 95% confidence interval [95% CI] 0.96–7.13) and high (32-Td-s: $5.20 \mu\text{V}$, 95% CI 1.54–8.86) retinal illuminance were lower in prediabetes, as were OCT-A parafoveal vessel densities in superficial ($0.051 \text{ pixels}/\text{mm}^2$, 95% CI 0.005–0.095) and deep ($0.048 \text{ pixels}/\text{mm}^2$, 95% CI 0.003–0.093) retinal layers. There were no differences in CCM or ESC measurements between these two groups. Correlations between HbA_{1c} and peak ERG amplitude at 32-Td-s ($r = -0.256$, $p = 0.028$), implicit time at 32-Td-s ($r = 0.422$, $p < 0.001$) and 16-Td-s ($r = 0.327$, $p = 0.005$), OCT parafoveal vessel density in the superficial ($r = -0.238$, $p = 0.049$) and deep ($r = -0.3$, $p = 0.017$) retinal layers, corneal nerve fibre length (CNFL) ($r = -0.293$, $p = 0.017$), and ESC-hands ($r = -0.244$, $p = 0.035$) were observed. HOMA-IR was a predictor of CNFD ($\beta = -0.94$, 95% CI -1.66 to -0.21 , $p = 0.012$) and CNBD ($\beta = -5.02$, 95% CI -10.01 to -0.05 , $p = 0.048$).

Conclusions: The glucose threshold for the diagnosis of diabetes is based on emergent retinopathy on fundus examination. We show that both abnormal

This is an open access article under the terms of the [Creative Commons Attribution-NonCommercial](https://creativecommons.org/licenses/by-nc/4.0/) License, which permits use, distribution and reproduction in any medium, provided the original work is properly cited and is not used for commercial purposes.

© 2022 The Authors. *Diabetic Medicine* published by John Wiley & Sons Ltd on behalf of Diabetes UK.

retinal neurovascular structure (OCT-A) and function (ERG) may precede retinopathy in prediabetes, which require confirmation in larger, adequately powered studies.

KEYWORDS

neuropathy-somatic, prediabetes, retinopathy

1 | INTRODUCTION

The management of diabetes and its long-term multiorgan morbidity remains a significant global health burden. In 2019, direct health expenditure for diabetes was an estimated \$760 billion worldwide.¹ Within 4 years of the diagnosis of diabetes, the global age- and sex-standardised prevalence of microvascular and macrovascular disease is 17.9%, compared to 9.2% in normoglycaemia.²

The current fasting glucose threshold of 7.0 mmol/L to diagnose diabetes is based on historical population-based data that correlated glycaemic variables with retinal abnormalities on fundus examination.³ However, the DETECT-2 (evaluation of screening and early detection strategies for type 2 diabetes and impaired glucose tolerance) collaboration recently reported the presence of diabetic retinopathy (DR) at a lower fasting plasma glucose of 6.5 mmol/L.⁴ There is growing recognition that diabetes-specific end-organ complications can develop prior to the onset of diabetes. Prediabetes is an established high-risk state for progression to diabetes.⁵ Worldwide, one in 13 adults (374 million) aged 20–79 years have prediabetes,⁶ with excess microvascular and macrovascular disease reported in these individuals compared with normoglycaemia.^{7,8}

New, highly sensitive diagnostic tools have demonstrated small nerve fibre damage and retinal neurodegeneration in prediabetes.⁹ Reduced sweating, measured using electrochemical skin conductance (ESC), shows sympathetic dysfunction in prediabetes,¹⁰ and corneal nerve parameters, measured using corneal confocal microscopy (CCM), are lower in subjects with impaired glucose tolerance who develop type 2 diabetes.¹¹ In addition to well-documented changes in the retinal nerve fibre layer detected with optical coherence tomography (OCT),¹² OCT-angiography (OCT-A) reveals a reduction in parafoveal vessel density, which precedes the onset of DR on fundus examination.¹³ Handheld electroretinography (ERG) data show that early retinal neurodysfunction can predict the onset of vision-threatening DR.¹⁴

This exploratory study compared the utility of OCT-A, handheld ERG, CCM and ESC for the detection of early neurovascular pathology in prediabetes and diabetes, to inform the selection of the most sensitive technologies to screen individuals at high risk of microvascular sequelae.

NOVELTY STATEMENT

What is already known?

- The glucose threshold for diabetes is historically based on the presence of retinopathy.
- Prediabetes is associated with micro- and macrovascular disease.

What this study has found?

- Handheld electroretinography and optical coherence tomography angiography can identify early retinal neurovascular dysfunction, in the absence of retinopathy on fundus imaging.

What are the implications of the study?

- Point-of-care devices may facilitate screening for early end-organ dysfunction in prediabetes, challenging current diagnostic thresholds for diabetes.

2 | METHODS

2.1 | Ethics statement

This study was approved by an independent National Health Service Research Ethics Committee in November 2018 (REC ID: 18/LO/2126). Written informed consent was obtained from all participants.

2.2 | Design, setting and population

Participants with prediabetes or type 2 diabetes were recruited from primary care, the South-East London Diabetic Eye Screening Programme (DESP) and diabetic eye clinics at a large teaching hospital (King's College Hospital). Pre-screening was conducted using primary care and hospital electronic patient record databases, and potentially eligible participants were invited to attend screening. Controls of similar ages with normoglycaemia were recruited through a King's College London research volunteer circular. In the absence of prior data, a sample

size of 25 per study group was chosen, based on consensus recommendations for exploratory analyses.¹⁵

2.3 | Eligibility criteria

Inclusion and exclusion criteria are listed in [Table 1](#).

2.4 | Study groups

Participants were stratified into three groups according to their HbA_{1c}: (i) normoglycaemia: <39 mmol/mol (5.7%), (ii) prediabetes: 39–47 mmol/mol (5.7–6.4%), and (iii) type 2 diabetes: >47 mmol/mol (>6.4%), as per American Diabetes Association criteria.

2.5 | Clinical and laboratory assessment

Participants completed questionnaires on their age, gender, ethnicity and date of diagnosis of either prediabetes or

type 2 diabetes, if relevant. Clinical examination included blood pressure, height, weight and waist circumference. Venous blood sampling was performed for fasting glucose, insulin, c-peptide, HbA_{1c}, renal function and lipid profile tests. Urine samples were collected to calculate the albumin-to-creatinine ratio (ACR). Homeostatic model assessment of insulin resistance (HOMA-IR) was calculated using the following equation:

$$\text{HOMA-IR} = \frac{\text{Fasting glucose} \left(\frac{\text{mmol}}{\text{L}} \right) \times \text{Fasting insulin} \left(\frac{\text{mIU}}{\text{ml}} \right)}{22.5}$$

2.6 | Handheld electroretinography

Handheld ERG was performed in each eye in no predetermined order by a masked examiner, using the RETeval device (LKC Technologies) ([Appendix S1](#)). Testing was conducted in a darkened room without pharmacological mydriasis. Implicit time and peak amplitude of responses were recorded in each eye in response to dim (16-Td.s) and bright (32-Td.s) retinal illumination. Pupil responses were also measured in photopic and scotopic conditions, to calculate the pupil area ratio.

2.7 | Optical coherence tomography angiography

After pharmacological mydriasis, images from both eyes were obtained in no predetermined order by a masked ophthalmic technician using the Heidelberg Spectralis OCT2/OCT-A (Heidelberg Engineering GmbH) ([Appendix S1](#)). Images from the superficial vascular plexus (SVP) and deep capillary plexus (DCP) were graded for quality by a masked examiner. Only images with <50% of the foveal avascular zone (FAZ) and parafoveal regions affected by motion artefacts were selected for analysis. The FAZ area was defined as the region surrounding the fovea devoid of any retinal capillaries on SVP images, using an automated method based on the Kanno-Saitama Image-J macro, implemented in MATLAB® (MathWorks; [Figure 1](#)). Where required, images were manually corrected by a masked examiner.

The parafoveal region was defined as the area bordered by two concentric rings with diameters of 1 and 2.5 mm centred on OCT-A images ([Figure 1e](#)). A validated, automated, object-oriented filtering vessel segmentation method was used to enhance and then binarise parafoveal SVP and DCP vessels. The parafoveal SVP and DCP vessel density was computed as the number of pixels occupied by the binarised vessels within the predefined ring region divided by the total area (mm²) of the predefined ring region ([Figure 1f](#)).

TABLE 1 Eligibility criteria

Inclusion criteria	Adults aged 18 years or older Able to comply with all study procedures and provide informed consent
Ocular exclusion criteria	Inability to obtain clear fundus imaging Any maculopathy or retinopathy of non-diabetic aetiology in either eye Previous macular laser therapy Intravitreal treatment or intraocular surgery within 3 months of enrolment Previous panretinal photocoagulation laser treatment Previous ocular trauma A known diagnosis of glaucoma, uveitis, or corneal disease in either eye, excluding any corneal abrasion that resolved spontaneously or with topical antibiotics taken for less than 1 month No restrictions on the severity of diabetic retinopathy or maculopathy for participants with type 2 diabetes
Systemic exclusion criteria	Photosensitive epilepsy Systemic vascular disease causing retinopathy Autoimmune disease or peripheral neuropathy of non-diabetic aetiology Pharmacotherapy known to interfere with electrochemical skin conductance within 48 h of testing

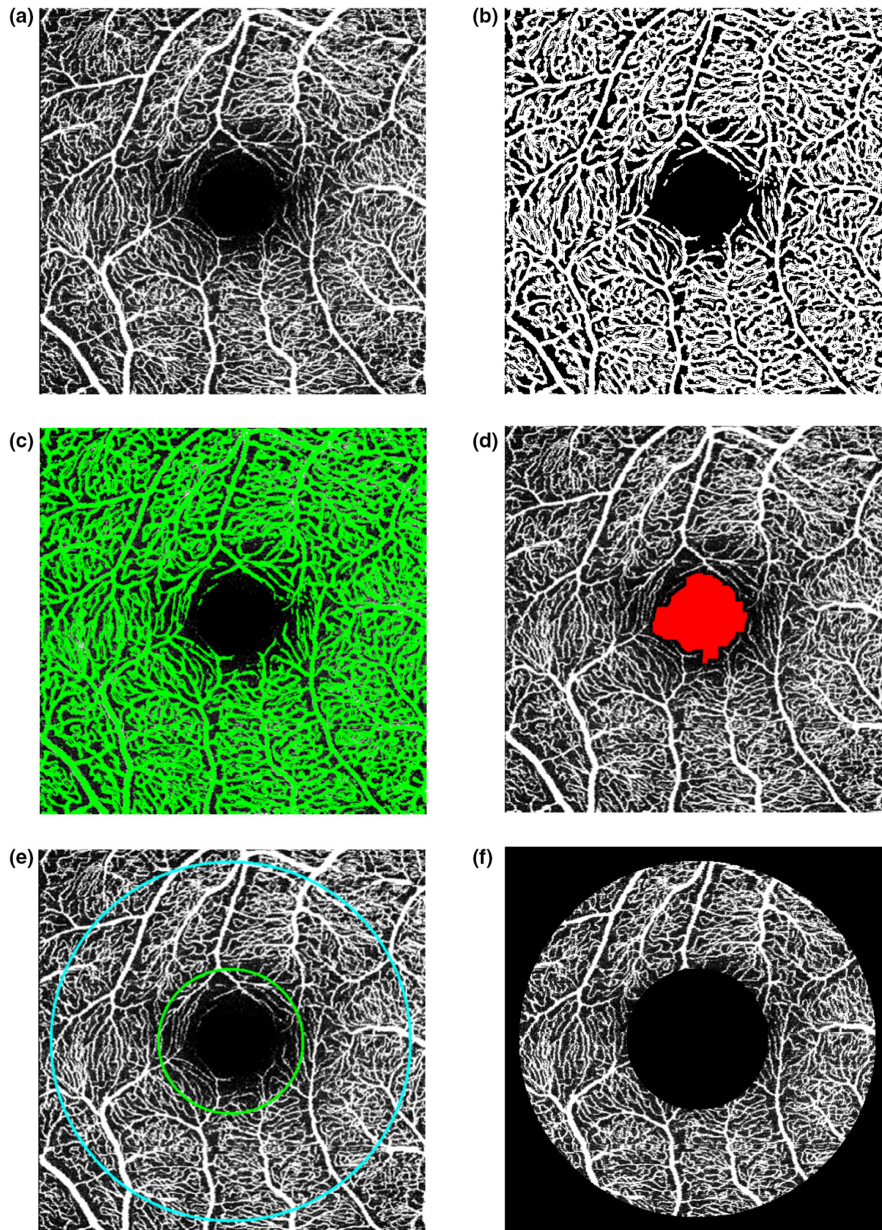


FIGURE 1 Optical coherence tomography angiography (OCT-A) image analysis protocol. Figures outline the image processing steps to calculate superficial vascular plexus (SVP) parafoveal vessel density and foveal avascular zone (FAZ) area: (a) raw OCT-A image, (b) binarised image after optimally oriented flux filtering and thresholding, (c) overlay of raw OCT-A image and binarised image, (d) FAZ area, (e) overlaid concentric rings with diameters of 1 mm (green) and 2.5 mm (blue) to define the parafoveal region, (f) the parafoveal region used to calculate vessel density by computing pixels against ring area.

2.8 | Corneal confocal microscopy

Both eyes of all participants were scanned with the Heidelberg Retinal Tomograph III Rostock Cornea Module (Heidelberg Engineering GmbH) in no predetermined order by a masked optometrist, using an established protocol (Appendix S1).¹⁶ Up to six central and eight inferior whorl (IW) images were selected equally from both eyes by a masked examiner, using previously reported criteria for image quality and location.¹⁷ Corneal nerves were traced using CCMetrics (University of Manchester, Manchester, UK) by two masked examiners, to obtain corneal nerve fibre length at the central cornea (CNFL-CC) or IW (CNFL-IW), corneal nerve fibre density, corneal nerve branch density and tortuosity coefficient.

2.9 | Electrochemical skin conductance

ESC was measured in both hands and feet of all participants by a masked examiner, and directly calculated using the SUDOSCAN device (Impeto Medical, Paris, France) (Appendix S1).

2.10 | Fundus photography

Dilated stereoscopic two-field colour fundus photography was performed by a masked ophthalmic technician. Images were obtained in no predetermined order of the macula and optic disc in each eye, using the Topcon TRC-50DX (Topcon Corporation). For participants with type 2 diabetes, images were also obtained from DESP

if performed within 4 weeks of enrolment. Images were graded as per UK National Screening Committee criteria.

2.11 | Test–retest variability

Reproducibility of ERG, OCT-A, CCM and ESC measurements have been described previously.^{10,13,14,16}

2.12 | Statistical analysis

Data were analysed using Stata/MP 16.0 (StataCorp). To focus on two-way comparisons, differences between groups were assessed using two-tailed t-tests instead of ANOVA, or Mann–Whitney tests, if data were parametric or non-parametric, respectively. Associations between systemic variables and microvascular parameters were explored using linear regression. The CCM measurements were averaged between both eyes, as per a validated protocol. In the absence of similar protocols for ESC, ERG and OCT-A, measurements for these technologies were analysed from the eye, hand, or foot, with the more abnormal reading. $p < 0.05$ were considered hypothesis-generating, hence adjustments were not made for multiple comparison testing. Regression analyses were performed, calculating standardised β -coefficients to report the unit change in the dependent variable in response to a single standard deviation change in the independent variable.

3 | RESULTS

3.1 | Enrolment and baseline characteristics

Of the 81 screened participants, three failed eligibility criteria, two were lost to follow-up and one withdrew participation. Based on HbA_{1c} results, seven previously undiagnosed participants were placed in the prediabetes group, whilst two participants with previously diagnosed prediabetes were placed in the type 2 diabetes group. This resulted in the following participant numbers: normoglycaemia ($n = 20$); prediabetes ($n = 29$); type 2 diabetes ($n = 26$).

3.2 | Clinical and laboratory data

Table 2 summarises the clinical and laboratory data for all participants, using means and medians for parametric and non-parametric data respectively. Differences in

waist circumference in males were noted between normoglycaemia and prediabetes (12.5 cm, 95% confidence interval [95% CI] 2.1–22.9) and between prediabetes and type 2 diabetes (9.2 cm, 95% CI 1.5–16.9); and in females, between normoglycaemia and type 2 diabetes (13.8 cm, 95% CI 0.4–27.2). There were also differences in systolic blood pressure (10.4 mmHg, 95% CI 1.5–19.2), HOMA-IR (0.89 units; $z = -2.81$, $p = 0.004$) and HDL (0.3 mmol/L; $z = 2.25$, $p = 0.02$) between normoglycaemia and type 2 diabetes, and in systolic blood pressure (9.0 mm Hg; 95% CI 0.9–17.0) and urinary ACR (0.04 mg/mmol; $z = -2.51$, $p = 0.01$) between prediabetes and type 2 diabetes.

Table 3 summarises parameters measured from all four technologies for all participants.

3.3 | Fundus photography

Dilated stereoscopic two-field colour fundus photography revealed no evidence of retinopathy in normoglycaemia or prediabetes. In type 2 diabetes, 15 (58%) and 11 (42%) participants had no DR (R0) and mild non-proliferative DR (R1) disease in the worse eye respectively. Among those with R1 disease, four participants had referable maculopathy (M1) disease in both eyes and three had M1 disease in one eye. None of the participants had referable moderate non-proliferative DR (R2) or worse in either eye.

3.4 | Handheld electroretinography

Measurable results were obtained on all 75 participants. Differences were observed in the peak amplitude of retinal responses at 32-Td·s in prediabetes (5.20 μ V, 95% CI 1.54–8.86) and type 2 diabetes (5.55 μ V, 95% CI 1.99–9.12), compared to normoglycaemia. A similar difference was also observed at 16-Td·s between normoglycaemia and prediabetes (4.04 μ V, 95% CI 0.96–7.13). The implicit time at 16-Td·s ($z = -2.96$, $p = 0.003$) and at 32-Td·s ($z = -3.53$, $p = 0.0003$) was longer in type 2 diabetes compared to prediabetes. There was a difference in implicit time between normoglycaemia and type 2 diabetes at 32-Td·s ($z = -2.71$, $p = 0.006$), but not at 16-Td·s ($z = -1.82$, $p = 0.07$). No differences were found in pupil area ratios in photopic and scotopic light conditions between groups. There was a trend for worsening peak amplitude and implicit time at both 16-Td·s and 32-Td·s, across all three groups, from normoglycaemia to type 2 diabetes (Cuzick's tests: $z = -2.09$, $p = 0.037$; $z = 2.01$, $p = 0.044$; $z = -2.42$, $p = 0.016$; $z = 2.81$, $p = 0.005$ respectively).

TABLE 2 Baseline characteristics of study participants

Baseline characteristic	Study group			p-value on two-way group comparisons		
	NGM	PD	T2DM	NGM vs PD	NGM vs T2DM	PD vs T2DM
Participants, <i>n</i>	20	29	26	—	—	—
Male sex, <i>n</i> (%)	9 (45.0)	16 (55.2)	15 (57.7)	—	—	—
Age (years)	55.3 (11.1)	61.0 (9.4)	60.7 (10.4)	0.06	0.10	0.92
Time since diagnosis of prediabetes or diabetes, <i>n</i>	—	<1 year: 6 1–5 years: 7 >5 years: 3 Unknown: 13	<1 year: 5 1–5 years: 10 >5 years: 9 Unknown: 2	—	—	—
Systolic blood pressure (mm Hg)	127.0* (16.6)	128.4[‡] (16.1)	137.4*[‡] (13.2)	0.76	0.02	0.03
Diastolic blood pressure (mm Hg)	84.7 (9.4)	86.0 (10.8)	88.6 (8.6)	0.66	0.15	0.33
Number of individuals taking antihypertensive medications, <i>n</i> (%)	5 [25]	10 [34]	13 [50]	—	—	—
Body mass index (kg/m ²)	26.1 (23.5–29.7)	27.5 (23.7–29.7)	28.9 (25.2–32.2)	0.79	0.20	0.29
Waist circumference in cm in males	104.3*[‡] (11.1)	91.9 (12.6)	101.1*[‡] (7.7)	0.02	0.40	0.02
Waist circumference in cm in females	80.4[†] (14.8)	87.7[†] (13.7)	94.2 (15.3)	0.22	0.04	0.29
Number of individuals taking statins, <i>n</i> (%)	2 (10)	9 (31)	14 (54)	—	—	—
HbA _{1c} in mmol/mol (%)	36*[†] (35–37) [5.4]	42[‡] (40–44) [6.0]	53*[‡] (49–58) [7.0]	<0.001	<0.001	<0.001
HOMA-IR (units)	1.55* (0.65–3.29)	2.13 (1.04–2.84)	2.44* (1.94–5.05)	0.28	0.004	0.09
Serum HDL (mmol/L)	1.6* (1.2–1.8)	1.4 (1.2–1.6)	1.3* (1.0–1.6)	0.23	0.03	0.17
Serum triglycerides (mmol/L)	1.0 (0.8–1.3)	1.2 (0.8–1.4)	1.1 (0.7–1.5)	0.35	0.66	0.61
eGFR (ml/min/1.73m ²)	83.5 (74.0–90.0)	79.0 (67.0–90.0)	80.5 (69.0–90.0)	0.32	0.51	0.77
Urinary ACR (mg/mmol)	0.58 (0.34–1.34)	0.63[‡] (0.35–1.42)	0.67[‡] (0.36–1.49)	0.96	0.08	0.01
Retinopathy on fundus image, <i>n</i> (%)	0 –	0 –	9 (35)	—	—	—

Notes: Participants divided by study group: (i) normoglycaemia (NGM), (ii) prediabetes (PD), and (iii) type 2 diabetes (T2DM). Parametric data are presented as means with standard deviations in parentheses; non-parametric data are presented as medians with interquartile ranges in parentheses. Other values are shown in square brackets.

Numbers in bold show statistically significant differences between groups.

Abbreviations: ACR, albumin–creatinine ratio; eGFR, estimated glomerular filtration rate; HDL, high-density lipoprotein; LDL, low-density lipoprotein.

$p < 0.05$ on two-tailed t-tests or Mann–Whitney tests shown by: * (NGM vs T2DM), [†] (NGM vs PD) and [‡] (PD vs T2DM).

3.5 | Optical coherence tomography angiography

After excluding ungradable images, data on FAZ area and vessel density in the SVP were available for 69 (92%) participants, and for the DCP in 63 (84%) participants, in at least one eye. Parafoveal vessel density was different in both the SVP (0.045 pixels/mm², $z = 2.64$, $p = 0.008$) and DCP (0.048 pixels/mm², 95% CI 0.003–0.093) between normoglycaemia and prediabetes. Between normoglycaemia and type 2 diabetes, SVP and DCP parafoveal vessel density both differed (0.050 pixels/mm², $z = 2.39$, $p = 0.016$; 0.068 pixels/mm², 95% CI 0.027–0.110 respectively). No differences were noted between prediabetes and type 2 diabetes. A difference in FAZ area was also observed between

normoglycaemia and type 2 diabetes (0.106 mm², 95% CI 0.019–0.193). There was a trend for increasing FAZ area, decreasing SVP and decreasing DCP parafoveal vessel density across all three groups, from normoglycaemia to type 2 diabetes (Cuzick's tests: $z = 2.58$, $p = 0.010$; $z = -2.35$, $p = 0.019$; $z = -2.91$, $p = 0.004$, respectively).

3.6 | Corneal confocal microscopy

Adequate CCM images were available for 71 (95%) participants. There were no differences between prediabetes and the other study groups; however, mean CNFL-CC was lower in type 2 diabetes compared to normoglycaemia (4.74 mm/mm², 95% CI 0.53–8.95).

TABLE 3 Neurovascular parameters of study participants

Microvascular parameter	Study group			p-value on two-way group comparisons		
	NGM	PD	T2DM	NGM vs PD	NGM vs T2DM	PD vs T2DM
<i>Handheld electroretinography</i>						
Peak amplitude at 16-Td-s (μ V)	19.4 [†] (5.6)	15.4 [†] (5.9)	15.9 (5.6)	0.01	0.05	0.70
Peak amplitude at 32-Td-s (μ V)	22.2 ^{*†} (6.4)	17.0 [†] (6.4)	16.7 [*] (6.1)	0.006	0.002	0.80
Implicit time at 16-Td-s (ms)	30.4 (29.2–32.2)	30.0 [‡] (28.6–31.2)	31.7 [‡] (30.6–33.8)	0.42	0.07	0.003
Implicit time at 32-Td-s (ms)	29.2 [*] (28.1–30.8)	28.9 [‡] (27.2–30.0)	31.1 ^{*‡} (29.8–31.9)	0.46	0.006	<0.001
Pupil area ratio (unitless)	1.70 (1.4–2)	1.70 (1.5–1.9)	1.80 (1.4–1.9)	0.86	0.69	0.79
<i>Optical coherence tomography angiography</i>						
FAZ area (mm^2)	0.298 [*] (0.134)	0.342 (0.134)	0.405 [*] (0.131)	0.22	0.02	0.07
SVP PVD (pixels/ mm^2)	0.477 ^{*†} (0.421–0.510)	0.432 [†] (0.341–0.468)	0.427 [*] (0.359–0.461)	0.008	0.02	0.98
DCP PVD (pixels/ mm^2)	0.411 ^{*†} (0.068)	0.363 [†] (0.070)	0.343 [*] (0.070)	0.04	0.002	0.30
<i>Corneal confocal microscopy</i>						
CNFL-CC (mm/mm^2)	30.63 [*] (6.80)	27.44 (6.85)	26.08 [*] (5.96)	0.15	0.04	0.46
CNFL-IW (mm/mm^2)	27.02 (7.44)	25.52 (7.77)	26.44 (5.92)	0.55	0.80	0.68
CNFD (fibres/ mm^2)	30.14 (5.91)	27.10 (6.21)	28.73 (7.44)	0.13	0.54	0.39
CNBD (branches/ mm^2)	85.94 (58.75–109.37)	103.54 (63.453–127.97)	93.75 (66.25–118.75)	0.43	0.53	0.76
TC (unitless)	16.74 (6.08)	17.74 (5.71)	17.65 (4.34)	0.60	0.59	0.95
<i>Electrochemical skin conductance</i>						
ESC-hands (μ S)	56.3 [*] (17.4)	51.1 (18.8)	44.8 [*] (19.1)	0.34	0.05	0.23
ESC-feet (μ S)	71.0 (51.5–80.0)	74.0 (58.0–79.0)	63.0 (55.0–72.0)	0.91	0.35	0.17

Note: Participants divided by study group: (i) normoglycaemia (NGM), (ii) prediabetes (PD) and (iii) type 2 diabetes (T2DM). Parametric data are presented as means with standard deviations in parentheses; non-parametric data are presented as medians with interquartile ranges in parentheses.

Numbers in bold show differences between groups.

Abbreviations: CC, central cornea; CNBD, corneal nerve branch density; CNFD, corneal nerve fibre density; CNFL, corneal nerve fibre length; DCP, deep capillary plexus; ESC, electrochemical skin conductance; FAZ, foveal avascular zone; IW, inferior whorl; PVD, parafoveal vessel density; SVP, superficial vascular plexus, TC, tortuosity coefficient.

$p < 0.05$ on two-tailed t-tests or Mann-Whitney tests shown by: * (NGM vs T2DM), [†] (NGM vs PD) and [‡] (PD vs. T2DM).

3.7 | Electrochemical skin conductance

Data were available for all 75 participants. There were no differences observed between normoglycaemia and prediabetes, although eight of 21 (38%) participants with severe ESC-hands deficits ($<40 \mu\text{S}$) and seven of 13 (54%) with severe ESC-feet deficits ($<50 \mu\text{S}$) had prediabetes. ESC-hands was lower ($11.45 \mu\text{S}$, 95% CI 0.15–22.76), but there was no difference in ESC-feet ($9.02 \mu\text{S}$, 95% CI -0.78 to 18.81) in with type 2 diabetes compared to normoglycaemia. There was a trend for worsening ESC-hands and ESC-feet across all three groups, from normoglycaemia to type 2 diabetes (Cuzick's tests: $z = -2.12$, $p = 0.034$; $z = -2.01$, $p = 0.045$ respectively).

3.8 | Correlation with HbA_{1c}

Figure 2 shows scatterplots of HbA_{1c} against the key parameters from each of the four technologies. There were

correlations between HbA_{1c} and CNFL ($r = -0.293$, $p = 0.017$), ESC-hands ($r = -0.244$, $p = 0.035$), peak amplitude at 32-Td-s ($r = -0.256$, $p = 0.028$), implicit time at 32-Td-s ($r = 0.422$, $p < 0.001$) and 16-Td-s ($r = 0.327$, $p = 0.005$), parafoveal vessel density in the SVP ($r = -0.238$, $p = 0.049$), and parafoveal vessel density in the DCP ($r = -0.3$, $p = 0.017$).

3.9 | Regression analysis

Table 4 displays regression coefficients (β) for the principal parameters from each of the four technologies against clinical and metabolic data. No patterns were observed on residual plots, hence a linear model was applied. In addition to associations with HbA_{1c}, both implicit time at 32-Td-s and DCP parafoveal vessel density showed associations with systolic blood pressure ($\beta = 0.04$, 95% CI 0–0.07, $p = 0.03$; $\beta = -0.001$, 95% CI -0.002 to 0, $p = 0.04$ respectively). HOMA-IR was a predictor of

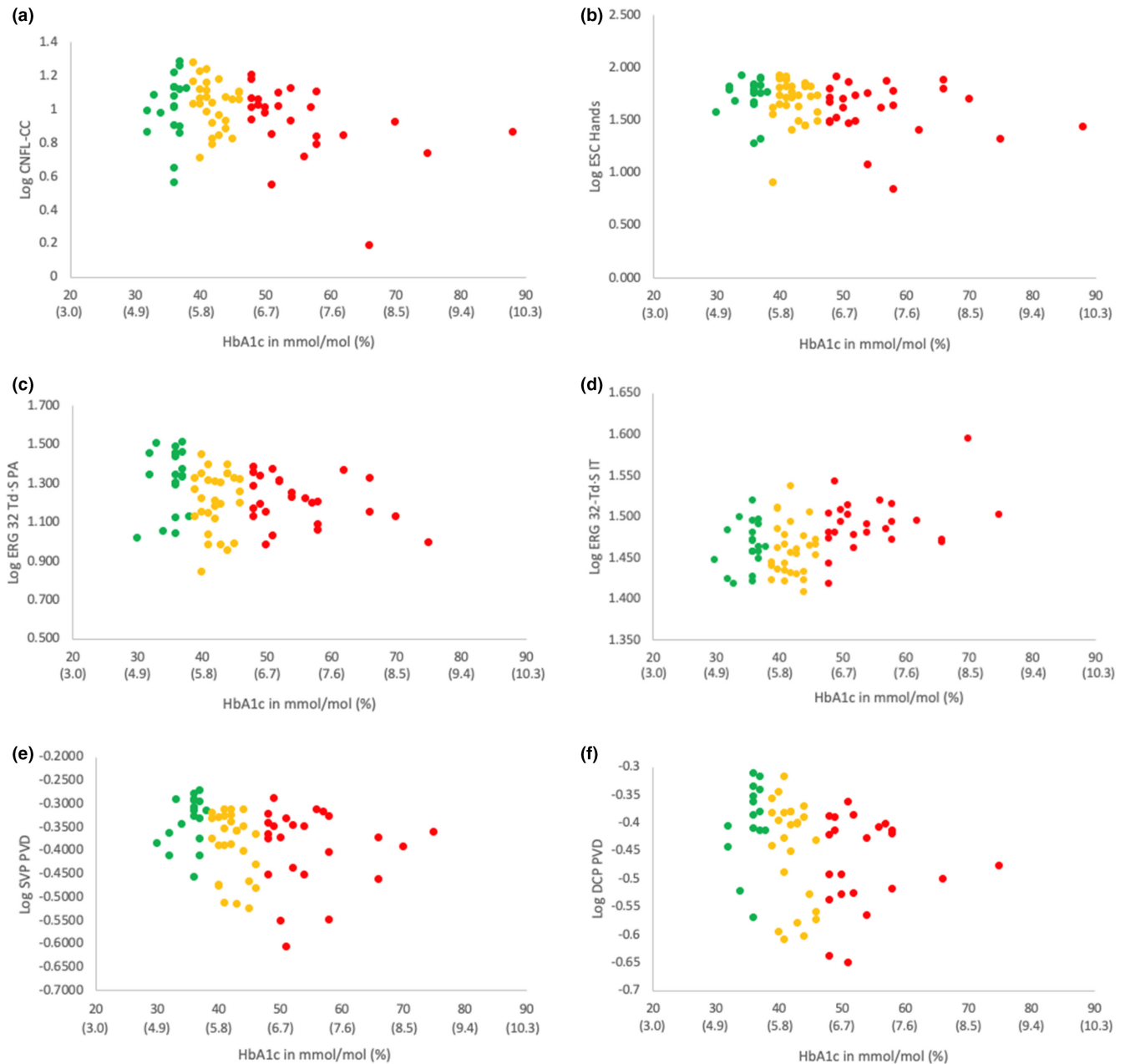


FIGURE 2 Scatterplots of microvascular parameters compared with HbA_{1c}. Data presented for (a) central cornea corneal nerve fibre length (CNFL-CC), (b) electrochemical sweat conductance (ESC) in the hands, (c) electroretinography (ERG) peak amplitude (PA) at 32-Td-S, (d) ERG implicit time (IT) at 32-Td-S, (e) superficial vascular plexus (SVP) parafoveal vessel density (PVD) and (f) deep capillary plexus (DCP) PVD. Data logarithmically transformed and colour-coded by study group: normoglycaemia (green), prediabetes (yellow) and type 2 diabetes (red).

CNFD ($\beta = -0.94$, 95% CI -1.66 to -0.21 , $p = 0.012$) and CNBD ($\beta = -5.02$, 95% CI -10.01 to -0.05 , $p = 0.048$), but not CNFL. The FAZ area was a predictor of SVP PVD ($\beta = -0.67$, 95% CI -1.12 to -0.21 , $p = 0.005$) and DCP PVD ($\beta = -0.7$, 95% CI -1.12 to -0.28 , $p = 0.001$). There was an association between implicit time at 32-Td-s and DCP parafoveal vessel density ($\beta = -8.8$, 95% CI -16.32 to -1.28 , $p = 0.02$). There were also associations between the FAZ area and ESC-hands ($\beta = -47.81$, 95% CI -80.9 to -14.74 , $p = 0.005$) and ESC-feet ($\beta = -53.2$, 95% CI -82.91 to -23.51 , $p < 0.001$).

4 | DISCUSSION

This study demonstrates that emerging, commercially available, retinal diagnostic devices may detect early end-organ damage in prediabetes. The abnormalities evident with handheld ERG and OCT-A suggest that retinal damage occurs prior to visible retinopathy. This challenges the current glycaemic thresholds for diabetes, that were set based on the detection of visible retinopathy.

Handheld ERG identified a reduction in peak amplitude of retinal responses and OCT-A showed reduced

TABLE 4 Regression analysis of key microvascular parameters

Variable	(a) Corneal confocal microscopy: CNFL-CC (μm)				(b) Electrochemical skin conductance: ESC-hands (μS)			
	Regression coefficient (β)	95% CI	p-value	Standardised β coefficient	Regression coefficient (β)	95% CI	p-value	Standardised β coefficient
Age (years)	-0.09	-0.26, 0.07	0.25	-0.14	-0.09	-0.52, 0.34	0.67	-0.05
SBP (mm Hg)	-0.04	-0.14, 0.07	0.49	-0.09	-0.03	-0.32, 0.25	0.81	-0.03
Waist (cm)	-0.11	-0.23, 0.00	0.06	-0.23	0.05	-0.26, 0.36	0.77	0.03
BMI (kg/m^2)	-0.28	-0.57, 0.02	0.06	-0.23	0.06	-0.71, 0.84	0.87	-0.02
HbA _{1c} (mmol/mol)	-0.18	-0.34, -0.30	0.02*	-0.29	-0.46	-0.87, -0.04	0.03*	-0.25
HOMA-IR	-0.68	-1.43, 0.07	0.07	-0.22	-0.87	-2.81, 1.07	0.38	-0.10
Variable	(c) Electroretinography: implicit time at 32-Td-s (ms)				(d) Optical coherence tomography angiography: DCP PVD ($\text{pixels}/\text{mm}^2$)			
	Regression coefficient (β)	95% CI	p-value	Standardised β coefficient	Regression coefficient (β)	95% CI	p-value	Standardised β coefficient
Age (years)	0.05	0.00, 0.10	0.06	0.22	-0.002	-0.003, 0.002	0.08	-0.22
SBP (mmHg)	0.04	0.00, 0.07	0.03*	0.25	-0.001	-0.002, 0.000	0.04*	-0.26
Waist (cm)	0.02	-0.02, 0.06	0.26	0.13	0.0006	-0.001, 0.002	0.34	0.12
BMI (kg/m^2)	0.04	-0.05, 0.14	0.39	0.10	0.0001	-0.003, 0.003	0.93	0.01
HbA _{1c} (mmol/mol)	0.11	0.06, 0.17	<0.001*	0.43	-0.003	-0.005, -0.007	0.009*	-0.33
HOMA-IR	0.06	-0.20, 0.33	0.63	0.06	-0.01	-0.01, 0.01	0.33	-0.12

Note: Regression coefficients (β) with 95% confidence intervals (95% CI) shown for (a) corneal nerve fibre length on the central cornea (CNFL-CC), (b) electrochemical skin conductance (ESC) in the hands, (c) implicit time at 32-Td-S and (d) deep capillary plexus parafoveal vessel density (DCP PVD).

Abbreviations: BMI, body mass index; HOMA-IR, homeostatic model assessment of insulin resistance; SBP, systolic blood pressure.

$p < 0.05$ shown by “*”. Standardised β coefficients display the predicted unit change in the dependent variable in response to a single standard deviation change in the independent variable.

parafoveal vessel density in the superficial (SVP) and deep (DCP) layers of the retina in the prediabetes group compared to normoglycaemia. In the EUROCONDOR study neurodysfunction, measured using multifocal ERG, was found in 60% of individuals with type 2 diabetes without visible DR.¹⁸ This is in keeping with published literature suggesting that retinal neurodegeneration precedes the onset of blood-retinal barrier breakdown and retinal vasculopathy. Indeed, Harrison et al. showed that multifocal ERG implicit time predicts the onset of DR in adults with diabetes.¹⁹ Furthermore, both ERG implicit time at 32-Td-s and DCP parafoveal vessel density were associated with HbA_{1c} and systolic blood pressure.

Whilst peak amplitude has been shown to be altered in individuals with mild-to-moderate hypertension, to our knowledge this is the first report of an association between systolic blood pressure and ERG implicit time.²⁰ Our data also suggest that retinal illuminance at 32-Td-s is a stronger discriminator of retinal dysfunction than 16-Td-s. Putative pathological mechanisms include retinal ischaemia secondary to focal retinal and choroidal circulatory

changes. The relatively low perfusion and high metabolic demands of the inner retina make it susceptible to metabolic stresses, with retinal ganglion cells among the first neuronal cells to undergo diabetes-induced apoptosis.

Hypertension has also been associated with a reduction in retinal capillary density in the deep rather than superficial vascular plexus.²¹ Similarly, vessel changes in the deep retinal layers are more significantly associated with the severity of DR and have a higher index to discriminate individuals with type 2 diabetes from controls.²² Ashraf et al. showed a differential reduction in vessel densities in the SVP and DCP, with greater involvement of the superficial retinal vasculature in advanced DR.²³ Frizziero et al. showed structural changes in the SVP and functional alterations of the mfERG in people with diabetes but no DR.²⁴ Our study corroborates emerging data that vessel density is a more sensitive measure of early retinal damage in dysglycaemia than FAZ area.²⁴

We did not find corneal nerve loss in prediabetes. This contrasts with previous studies showing corneal nerve loss in subjects with IGT and increased neuropathic

symptoms, increased thermal thresholds, and reduced intraepidermal nerve fibre density.¹¹ These data suggest a spectrum of small nerve fibre dysfunction and damage in people with prediabetes, and may be related to the lower-than-expected BMI of the prediabetes group.⁹ Indeed, we have recently demonstrated corneal nerve loss in obese individuals without diabetes, which improved after bariatric surgery.²⁵ We found a tendency for greater corneal nerve loss with increasing waist size, BMI and HOMA-IR. We have also previously shown a reduction in corneal nerve fibre density but no difference in corneal nerve fibre length or branch density in patients with screen detected type 2 diabetes and good glycaemic control.²⁶ We found no evidence of sudomotor dysfunction in subjects with prediabetes in contrast with previous data,¹⁰ and more marked abnormalities in the hands as opposed to the feet in patients with type 2 diabetes.

Limitations of the current dataset include the relatively high waist circumference and BMI of normoglycaemic controls, particularly males. This was in part due to difficulties in recruiting non-obese individuals of similar ages, along with unanticipated HbA_{1c} results and group allocation. Despite the relatively small sample size and lack of corroborative tests to categorise dysglycaemia (IFG, IGT or both), between-group differences were demonstrated alongside associations with HbA_{1c}, blood pressure and insulin resistance. The data generated provide a compelling rationale for larger, adequately powered studies to confirm or refute our findings. Additionally, longitudinal studies are required to assess the utility of these measures in identifying individuals most likely to develop progressive microvascular disease.

There are emerging data that early interventions in at-risk individuals can prevent the progression of microvascular complications. Lifestyle interventions including diet and exercise and randomised controlled trials of new antidiabetic medications have all shown benefits.²⁷ We recently demonstrated that treatment with GLP-1 or insulin in patients with type 2 diabetes leads to an improvement in corneal nerve morphology.²⁸ In a follow-up to the EUROCONDOR study, topical administration of brimonidine and somatostatin as neuroprotective agents prevented the worsening of retinal neurodysfunction.²⁹

A one-stop microvascular screening service using point-of-care devices may provide a feasible model for the early detection and follow-up of neurovascular disease in prediabetes and type 2 diabetes, and warrants further investigation.³⁰ The presence of early end-organ damage could be used to individualise the diagnostic thresholds between normoglycaemia, prediabetes and diabetes, rather than relying solely on measures of hyperglycaemia. The two most promising devices tested in this study could be easily adapted to screen people with prediabetes.

Handheld ERG is relatively inexpensive, portable, easy to use, does not require pupillary dilatation and could be undertaken rapidly in most clinical settings. OCT-A is expensive, requires a trained technician and requires pupillary dilatation, but is now routinely available in most hospital eye clinics.

In summary, rapid, non-invasive and commercially available devices can identify early retinal neurovascular damage in individuals with prediabetes.

AUTHOR CONTRIBUTIONS

VK, UA, PV, DH and TLJ were responsible for conceptualisation, investigation and methodology. KIR, KA, BPZ, BC, SH and VK were responsible for data curation. FAS, INP, RAM, TP and ChB were responsible for device-specific, blinded data analysis. Statistical analysis was conducted by VK, PN and BPZ, with CaB providing senior oversight. VK, KIR, KA and BPZ all directly accessed and verified the underlying data reported in the manuscript. VK was responsible for project administration, resource management and software acquisition. VK, PN, UA and BPZ were responsible for writing the original draft. All other authors each contributed to manuscript review and editing prior to submission. As guarantor, TLJ accepts full responsibility for the work and/or the conduct of the study, had access to the data and controlled the decision to publish.

ACKNOWLEDGEMENT

We acknowledge the expertise provided by the following individuals in device set-up and data analysis: Chris Mody from Heidelberg Engineering UK, Karin Feit and Jan McMeekin from Welch Allyn Europe, and Quentin Davis and James Datovech from LKC Technologies Inc. We are grateful to the staff at King's College Hospital and Moorfields Eye Hospital, without whom this study would not have been possible. We also extend our gratitude to Prof Lyndon Da Cruz of Moorfields Eye Hospital London and University College London for his funding of the Robotics and Vision Lab that conducted the OCT-A image analysis.

FUNDING INFORMATION

This research received no specific grant from any funding agency in the public, commercial or not-for-profit sectors.

CONFLICT OF INTEREST

None of the authors have any relevant financial disclosures to declare. LKC Technologies Inc. and Impeto Medical Inc. provided free use of the RETeval and SUDOSCAN devices, respectively, for this study. PN is funded by Diabetes UK. CaB is part-funded by the National Institute for Health Research (NIHR) Biomedical Research Centre at The Royal Marsden NHS Foundation Trust and the Institute of

Cancer Research, London. The views expressed are those of the author(s) and not necessarily those of Diabetes UK, the NIHR or the Department of Health and Social Care.

DATA AVAILABILITY STATEMENT

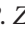
The datasets generated during and/or analysed during the current study are available from the corresponding author on reasonable request.

ORCID

Varo Kirthi  <https://orcid.org/0000-0003-4322-1017>

Kate I. Reed  <https://orcid.org/0000-0002-4112-4881>

Komeil Alattar  <https://orcid.org/0000-0002-2427-0449>

Benjamin P. Zuckerman  <https://orcid.org/0000-0002-0077-6074>

Catey Bunce  <https://orcid.org/0000-0002-0935-3713>

Paul Nderitu  <https://orcid.org/0000-0002-8571-0751>


Uazman Alam  <https://orcid.org/0000-0002-3190-1122>

Scott Hau  <https://orcid.org/0000-0001-6913-6107>

Fatima Al-Shibani  <https://orcid.org/0000-0002-8309-086X>

Ioannis N. Petropoulos  <https://orcid.org/0000-0002-1126-7638>

Rayaz A. Malik  <https://orcid.org/0000-0002-7188-8903>

Theodoros Pissas  <https://orcid.org/0000-0001-9500-7085>

Christos Bergeles  <https://orcid.org/0000-0002-9152-3194>

Prashanth Vas  <https://orcid.org/0000-0001-7448-2995>

David Hopkins  <https://orcid.org/0000-0002-0451-0900>

Timothy L. Jackson  <https://orcid.org/0000-0001-7618-1555>

REFERENCES

- Williams R, Karuranga S, Malanda B, et al. Global and regional estimates and projections of diabetes-related health expenditure: results from the International Diabetes Federation Diabetes Atlas, 9th edition. *Diabetes Res Clin Pract.* 2020;162:108072. doi:10.1016/j.diabres.2020.108072
- Kosiborod M, Gomes MB, Nicolucci A, et al. Vascular complications in patients with type 2 diabetes: prevalence and associated factors in 38 countries (the DISCOVER study program). *Cardiovasc Diabetol.* 2018;17(1):150. doi:10.1186/s12933-018-0787-8
- The Expert Committee on the Diagnosis and Classification of Diabetes Mellitus. Report of the Expert Committee on the diagnosis and classification of diabetes mellitus. *Diabetes Care.* 1997;20(7):1183-1197. doi:10.2337/diacare.20.7.1183
- Colagiuri S, Lee CMY, Wong TY, et al. Glycemic thresholds for diabetes-specific retinopathy: implications for diagnostic criteria for diabetes. *Diabetes Care.* 2011;34(1):145-150. doi:10.2337/dc10-1206
- Tabák AG, Herder C, Rathmann W, Brunner EJ, Kivimäki M. Prediabetes: a high-risk state for diabetes development. *The Lancet.* 2012;379(9833):2279-2290. doi:10.1016/S0140-6736(12)60283-9
- Center for Disease Control and Prevention. Prediabetes—Your chance to prevent type 2 diabetes. Published online June 11, 2020. Accessed November 1, 2020. <https://www.cdc.gov/diabetes/basics/prediabetes.html>
- Vistisen D, Witte DR, Brunner EJ, et al. Risk of cardiovascular disease and death in individuals with prediabetes defined by different criteria: the Whitehall II study. *Diabetes Care.* 2018;41(4):899-906. doi:10.2337/dc17-2530
- Kirthi V, Perumbalath A, Brown E, et al. Prevalence of peripheral neuropathy in pre-diabetes: a systematic review. *BMJ Open Diabetes Res Care.* 2021;9(1):e002040. doi:10.1136/bmjdr-2020-002040
- Asghar O, Petropoulos IN, Alam U, et al. Corneal confocal microscopy detects neuropathy in subjects with impaired glucose tolerance. *Diabetes Care.* 2014;37(9):2643-2646. doi:10.2337/dc14-0279
- Yang Z, Xu B, Lu J, et al. Autonomic test by EZSCAN in the screening for prediabetes and diabetes. *PLoS One.* 2013;8(2):e56480. doi:10.1371/journal.pone.0056480
- Azmi S, Ferdousi M, Petropoulos IN, et al. Corneal confocal microscopy identifies small-fiber neuropathy in subjects with impaired glucose tolerance who develop type 2 diabetes. *Diabetes Care.* 2015;38(8):1502-1508. doi:10.2337/dc14-2733
- De Clerck EEB, Schouten JSAG, Berendschot TTJM, et al. Macular thinning in prediabetes or type 2 diabetes without diabetic retinopathy: the Maastricht Study. *Acta Ophthalmol.* 2018;96(2):174-182. doi:10.1111/aos.13570
- Li Z, Alzogool M, Xiao J, Zhang S, Zeng P, Lan Y. Optical coherence tomography angiography findings of neurovascular changes in type 2 diabetes mellitus patients without clinical diabetic retinopathy. *Acta Diabetol.* 2018;55(10):1075-1082. doi:10.1007/s00592-018-1202-3
- Maa AY, Feuer WJ, Davis CQ, et al. A novel device for accurate and efficient testing for vision-threatening diabetic retinopathy. *J Diabetes Complications.* 2016;30(3):524-532. doi:10.1016/j.jdiacomp.2015.12.005
- Sim J, Lewis M. The size of a pilot study for a clinical trial should be calculated in relation to considerations of precision and efficiency. *J Clin Epidemiol.* 2012;65(3):301-308. doi:10.1016/j.jclinepi.2011.07.011
- Kalteniece A, Ferdousi M, Adam S, et al. Corneal confocal microscopy is a rapid reproducible ophthalmic technique for quantifying corneal nerve abnormalities. *PLoS ONE.* 2017;12(8):e0183040. doi:10.1371/journal.pone.0183040
- Petropoulos IN, Manzoor T, Morgan P, et al. Repeatability of in vivo corneal confocal microscopy to quantify corneal nerve morphology. *Cornea.* 2013;32(5):e83-e89. doi:10.1097/ICO.0b013e3182749419
- Santos AR, Ribeiro L, Bandello F, et al. Functional and structural findings of neurodegeneration in early stages of diabetic retinopathy: cross-sectional analyses of baseline data of the EUROCONDOR project. *Diabetes.* 2017;66(9):2503-2510. doi:10.2337/db16-1453
- Harrison WW, Bearse MA, Ng JS, et al. Multifocal electroretinograms predict onset of diabetic retinopathy in adult patients with diabetes. *Invest Ophthalmol Vis Sci.* 2011;52(2):772-777. doi:10.1167/iovs.10-5931
- Gundogan FC, Isilak Z, Erdurman C, Mumcuoglu T, Durukan AH, Bayraktar MZ. Multifocal electroretinogram in mild to moderate essential hypertension. *Clin Exp Hypertens.* 2008;30(5):375-384. doi:10.1080/10641960802275148

21. Chua J, Chin CWL, Hong J, et al. Impact of hypertension on retinal capillary microvasculature using optical coherence tomographic angiography. *J Hypertens*. 2019;37(3):572-580. doi:10.1097/HJH.0000000000001916
22. Chen Q, Ma Q, Wu C, et al. Macular vascular fractal dimension in the deep capillary layer as an early indicator of microvascular loss for retinopathy in type 2 diabetic patients. *Invest Ophthalmol Vis Sci*. 2017;58(9):3785-3794. doi:10.1167/iops.17-21461
23. Ashraf M, Sampani K, Clermont A, et al. Vascular density of deep, intermediate and superficial vascular plexuses are differentially affected by diabetic retinopathy severity. *Invest Ophthalmol Vis Sci*. 2020;61(10):53. doi:10.1167/iops.61.10.53
24. Frizziero L, Midena G, Longhin E, et al. Early retinal changes by OCT angiography and multifocal electroretinography in diabetes. *J Clin Med*. 2020;9(11):3514. doi:10.3390/jcm9113514
25. Azmi S, Ferdousi M, Liu Y, et al. Bariatric surgery leads to an improvement in small nerve fibre damage in subjects with obesity. *Int J Obes (Lond)*. 2021;45(3):631-638. doi:10.1038/s41366-020-00727-9
26. Andersen ST, Grosen K, Tankisi H, et al. Corneal confocal microscopy as a tool for detecting diabetic polyneuropathy in a cohort with screen-detected type 2 diabetes: ADDITION-Denmark. *J Diabetes Complications*. 2018;32(12):1153-1159. doi:10.1016/j.jdiacomp.2018.09.016
27. Braga T, Kraemer-Aguiar LG, Docherty NG, Le Roux CW. Treating prediabetes: why and how should we do it? *Minerva Med*. 2019;110(1):52-61. doi:10.23736/S0026-4806.18.05897-4
28. Ponirakis G, Abdul-Ghani MA, Jayyousi A, et al. Effect of treatment with exenatide and pioglitazone or basal-bolus insulin on diabetic neuropathy: a substudy of the Qatar Study. *BMJ Open Diabetes Res Care*. 2020;8(1):e001420. doi:10.1136/bmjdr-2020-001420
29. Simó R, Hernández C, Porta M, et al. Effects of topically administered neuroprotective drugs in early stages of diabetic retinopathy: results of the EUROCONDOR clinical trial. *Diabetes*. 2019;68(2):457-463. doi:10.2337/db18-0682
30. Binns-Hall O, Selvarajah D, Sanger D, Walker J, Scott A, Tesfaye S. One-stop microvascular screening service: an effective model for the early detection of diabetic peripheral neuropathy and the high-risk foot. *Diabet Med*. 2018;35(7):887-894. doi:10.1111/dme.13630

SUPPORTING INFORMATION

Additional supporting information can be found online in the Supporting Information section at the end of this article.

How to cite this article: Kirthi V, Reed KI, Alattar K, et al. Multimodal testing reveals subclinical neurovascular dysfunction in prediabetes, challenging the diagnostic threshold of diabetes. *Diabet Med*. 2022;00:e14952. doi: [10.1111/dme.14952](https://doi.org/10.1111/dme.14952)